

Transverse Component in the Longitudinal Asymmetry
for the Backward Running Phase of the
 G^0 Experiment

J. M. Mammei*

Virginia Tech

Contents

1	Introduction	4
2	The Transverse Asymmetry Correction	4
2.1	The A_T During Longitudinal Running	5
2.2	Measuring the Transverse Asymmetry	7
2.3	Correction or Uncertainty?	12
3	Summary and Conclusion	14
A	Wein Angle Settings	16

List of Figures

1	Spin dance for 687MeV run period in October 2006.	6
2	The H362 longitudinal asymmetry, fit with the phase free to vary.	7
3	The layout of the luminosity monitors.	7
4	The raw luminosity monitor asymmetries during transverse runs, vs. octant.	8
5	The background asymmetry corrected electron transverse asymmetries, vs. ϕ	8
6	The octant definition relative to ϕ in the backward angle running.	10
7	View of the ferris wheel from downstream.	10
8	An example of the octant to octant yield variation in the D687 dataset.	12
9	Theory calculation at different energies vs. lab scattering angle.	13
10	An example of how the spin precesses through the accelerator.	17

List of Tables

1	Summary of the magnitude of the transverse asymmetries in each dataset. . .	9
2	Summary of the phases from free fits to the LUMI and detector data.	11
3	Summary of the magnitude of the transverse correction in each dataset. . . .	15
4	Summary of the wien angle settings for each dataset.	18

1 Introduction

This document describes the method for estimating the transverse component of the longitudinal asymmetry. The correction is small ($< 1ppm$), and as it turns out we don't actually correct the data for the value, but rather include it as an additional systematic uncertainty. In the limit of perfectly symmetric detectors the contribution from any transverse component would disappear when we look at average of the octants. If the detectors are not perfectly symmetric then the transverse component can give an additive correction to the measured asymmetry.

2 The Transverse Asymmetry Correction

The transverse asymmetries are a parity *conserving* asymmetry that arises due to the interference of 2γ exchange with that of a single photon [3], and this beam normal single spin asymmetry can be written:

$$\begin{aligned} B_n = & \frac{2m_e}{Q} \sqrt{2\epsilon(1-\epsilon)} \sqrt{1 + \frac{1}{\tau}} (G_M^2 + \frac{\epsilon}{\tau} G_E^2)^{-1} \\ & \times \left\{ -\tau G_M \mathfrak{S}(\tilde{F}_3 + \frac{1}{1+\tau} \frac{\nu}{M^2} \tilde{F}_5) - G_E \mathfrak{S}(\tilde{F}_4 + \frac{1}{1+\tau} \frac{\nu}{M^2} \tilde{F}_5) \right\} \\ & + \mathcal{O}(e^4) \end{aligned} \tag{1}$$

For an arbitrary polarization, the measured asymmetry has a component from the parity violating asymmetry (A_{PV}) and the parity conserving asymmetry ($\epsilon(\phi)$). In order to separate the contributions, it is necessary to measure the asymmetry at two different polarizations. In practice the measurement is made when the beam is essentially longitudinal, and then in a mode where it is essentially transverse, and the contributions to the asymmetry can be written [2]

$$\begin{aligned}
A_{PV} &= \frac{\cos\beta}{P_{\parallel}\cos(\alpha - \beta)}A_m^{\parallel} - \frac{\sin\alpha}{P_{\perp}\cos(\alpha - \beta)}A_m^{\perp} \\
\epsilon(\phi) &= \frac{\sin\beta}{P_{\parallel}\cos(\alpha - \beta)}A_m^{\parallel} + \frac{\cos\alpha}{P_{\perp}\cos(\alpha - \beta)}A_m^{\perp}
\end{aligned} \tag{2}$$

where P_{\parallel} and P_{\perp} are the values of the polarization during the longitudinal and transverse running modes. In the case of the G0 backward angle running the polarizations in each mode are approximately equal [4], so we take $P_{\parallel} \approx P_{\perp}$. $\alpha = \theta_{spin}$ and $\beta = \theta'_{spin} - \frac{\pi}{2}$ are the angles that the spin is different from purely longitudinal or purely transverse during those modes, and A_m^{\parallel} and A_m^{\perp} are the measured longitudinal and transverse asymmetries. Thus we have:

$$\begin{aligned}
A_{PV} &= \frac{1}{P\cos(\alpha - \beta)}(A_m^{\parallel}\cos\beta - A_m^{\perp}\sin\alpha) \\
\epsilon(\phi) &= \frac{1}{P\cos(\alpha - \beta)}(A_m^{\parallel}\sin\beta + A_m^{\perp}\cos\alpha)
\end{aligned} \tag{3}$$

So, for example, if the spin were perfectly aligned in each mode, then $\alpha=\beta=0$, and you would only need to correct the measured longitudinal asymmetry, A_m^{\parallel} for the measured polarization, and similarly for the transverse asymmetry. In practice α and β are small, but not necessarily zero.

2.1 The A_T During Longitudinal Running

There are a couple of ways that the transverse component during longitudinal running can be approximated. The longitudinal polarization is measured at various wien angle settings

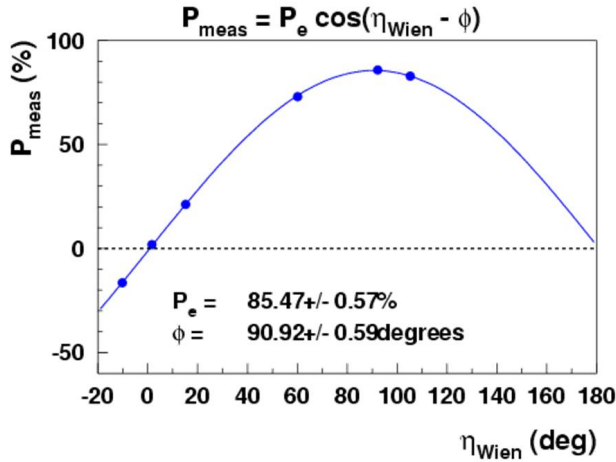


Figure 1: Spin dance for 687MeV run period in October 2006.

(a *spin dance*). Because the moller polarimeter only measures longitudinal polarization, the deviation from the maximum polarization gives you an idea of the size of the transverse component of the beam. Figure 1 shows the spin dance for 687 MeV done in October 2006. The maximum polarization is at a wien angle setting of 90.92° . The polarization crosses zero at about 1.7° , so this would be the ideal setting for the transverse running. A table of the actual wien angle settings for each run period is given in appendix A.

In addition to the polarization measurements, which help to determine the optimum wien angle setting, it is actually possible to see the sinusoidal variation caused by the transverse component of the beam in the data (see Figure 3), and in the luminosity monitors, even when it is not visible in the data, because they have such high rates. See Figure 3 for a description of the LUMI layout relative to the main detectors. Note also that the lumi monitors need to be properly ordered in order to match the octants.

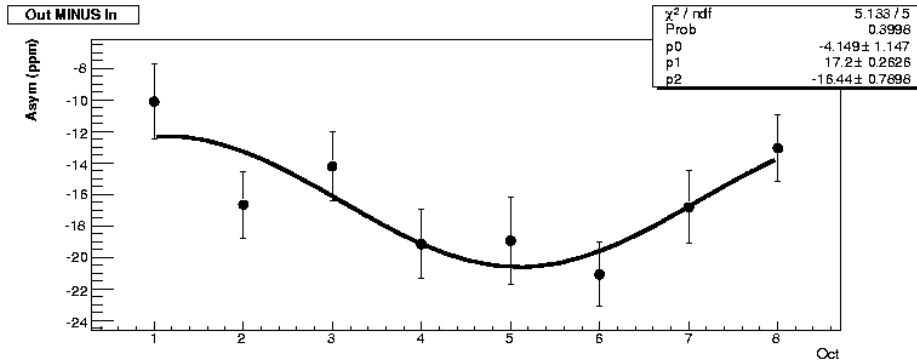


Figure 2: The H362 longitudinal asymmetry, fit with the phase free to vary.

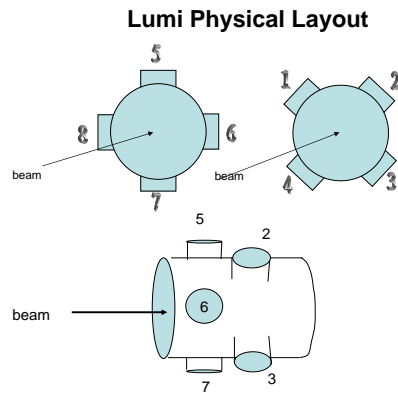


Figure 3: The layout of the luminosity monitors.

2.2 Measuring the Transverse Asymmetry

In order to estimate the size of the correction to the asymmetry you need to know the size of the transverse asymmetry in the main detectors (see Figure 5) and in the luminosity monitors (Figure 4). So at each target energy combination dedicated transverse runs were

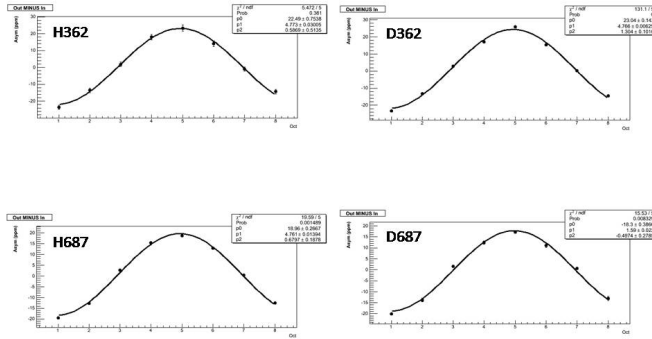


Figure 4: The raw luminosity monitor asymmetries during transverse runs, vs. octant.

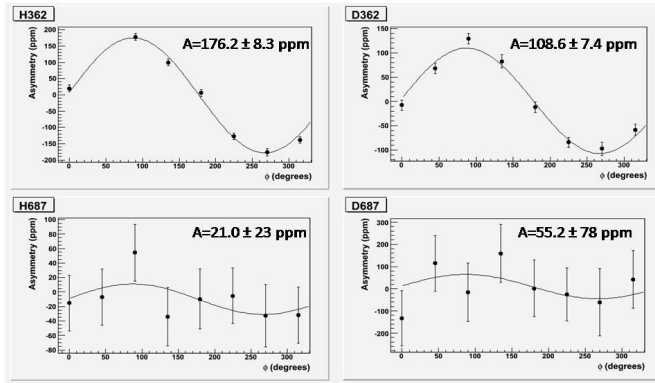


Figure 5: The background asymmetry corrected electron transverse asymmetries, vs. ϕ .

taken, for a total of about 50 hours of beam. The results are summarized in Table 2.2. The detector phases were fixed to the weighted average of the 362 MeV detector phases, as will

Dataset	Asymmetry	Offset (ppm)	$\frac{\chi^2}{ndf}$ (ppm)
H362	176.2 ± 8.7	-1.7 ± 4	1.9
D362	108.6 ± 7.6	1.4 ± 4	1.6
H687	21.0 ± 23	-9.9 ± 14	0.4
D687	55.2 ± 78	10 ± 46	0.5

Table 1: Summary of the magnitude of the transverse asymmetries in each dataset.

be discussed below.

The measured asymmetry is a function of the beam normal spin asymmetry and has a sinusoidal dependence on octant number because of the relationship between the polarization vector and the normal to the scattering plane:

$$A_{\perp}^m = \frac{\sigma_{\uparrow} - \sigma_{\downarrow}}{\sigma_{\uparrow} + \sigma_{\downarrow}} = A_n \vec{p}_e \cdot \hat{n} = -A_n \sin(\phi + \phi_o) \quad (4)$$

The angle of the spin out of plane, ϕ , is defined as being zero to beam left when looking downstream, see Figure 6. In the backward angle running, octant 3 is in the beam left position, then clockwise from beam left is 2, 1, 8, 7, 6, 5, and 4 see Figure 7.

As discussed in Appendix A, the out of plane component is very small, so the phase is expected to be small. In the plots versus octant the phase is $90^\circ \pm \delta$ where δ could be from an actual out of plane phase of the electron's spin, or it could be a geometrical phase of the detector. The phases from sinusoidal fits of the LUMI and main detector data, where the phases were allowed to be vary in addition to the amplitude and offset, are shown in Table

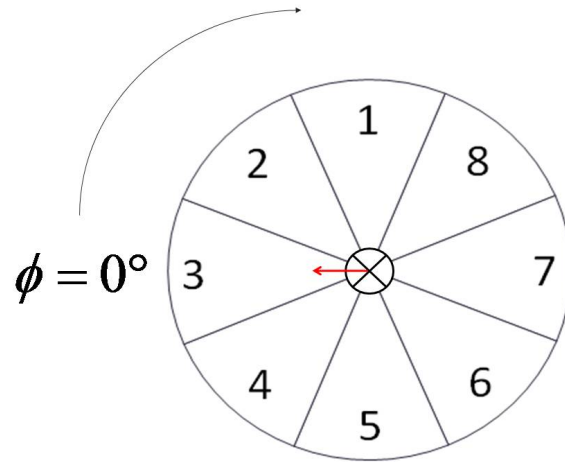


Figure 6: The octant definition relative to ϕ in the backward angle running.



Figure 7: View of the ferris wheel from downstream.

Dataset	LUMI Phase (degrees)	Detector Phase (degrees)
H362	-86.5 ± 1.7	-92.6 ± 1.9
D362	-86.9 ± 0.4	-91.6 ± 3.4
H687	-87.2 ± 0.8	-79.1 ± 68
D687	-88.9 ± 1.3	-66.2 ± 63

Table 2: Summary of the phases from free fits to the LUMI and detector data.

2.2. The LUMI data are essentially consistent with each other, and likewise the detector data are consistent, though the higher energy phases have large errors. But the LUMI phase is not consistent with the main detector phase. I believe this is because of an actual geometrical offset between the main detectors and the LUMIs. Both are close to 90° , as expected. There is no physics that would explain a difference in phase between the two sets of detectors.

The consistency of the LUMI phases from dataset to dataset gives some confidence that whatever out of plane phase of the electron's spin existed was the same in each dataset. Because I believe that there may be a geometrical offset between the LUMIs and the main detectors, however, I chose to use the weighted average of the phases at the lower energy in order to fix the phases of the sinusoidal fits to the main detector data in each data set. The value of δ , the difference from 90° of the weighted average of the phases of the main detectors at the lower energy setting is $-2.3^\circ \pm 1.6^\circ$. The main detector plots in 5 reflect this choice of phase. The difference in phase in a plot vs. octant and a plot vs. phi involves a 90° rotation as well as a reversal of order, so the $-\delta$ becomes the value of the phase, or 2.3° .

2.3 Correction or Uncertainty?

In order to estimate the size of the correction, K_T , it is necessary to know the value of the detector asymmetry, A_S :

$$K_T = A_T \frac{P_T}{P} A_S \quad (5)$$

where A_T is the amplitude of the transverse asymmetry $\epsilon(\phi)$ and $\frac{P_T}{P}$ is the relative transverse polarization in the longitudinal running. This ratio can be found by comparing the amplitudes of sin fits for the LUMIs in longitudinal and transverse running. The LUMI transverse amplitudes are also summarized in Table 3.

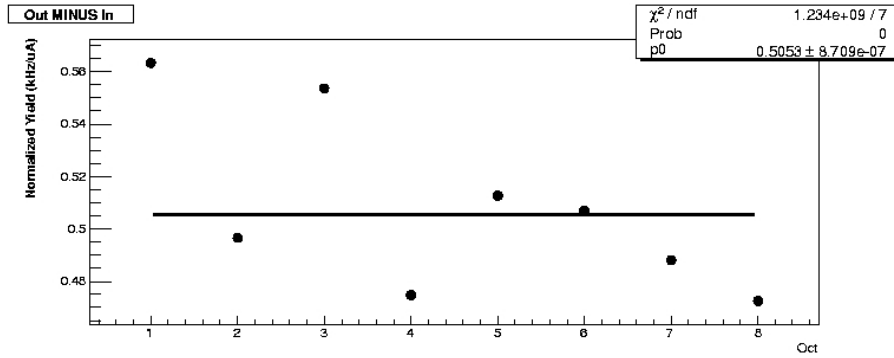


Figure 8: An example of the octant to octant yield variation in the D687 dataset.

An estimate of the detector asymmetry, A_S , can be made using the variation in the yields from octant to octant [5]. Figure 8 shows an example of the variation of the yields from octant to octant. The variation is about $\pm 6\%$ around the mean yield. If you assume that all of the variation comes from a difference in the scattered electron angle (surely an overestimate) then you can make an estimate about how much the transverse asymmetry would vary from octant to octant. Figure 9 shows a prediction for the magnitude of the transverse asymmetry for various energies as a function of lab scattering angle by Pasquini

and Vanderhaeghen [3]. This theory closely matches the available data for backward angles [6].

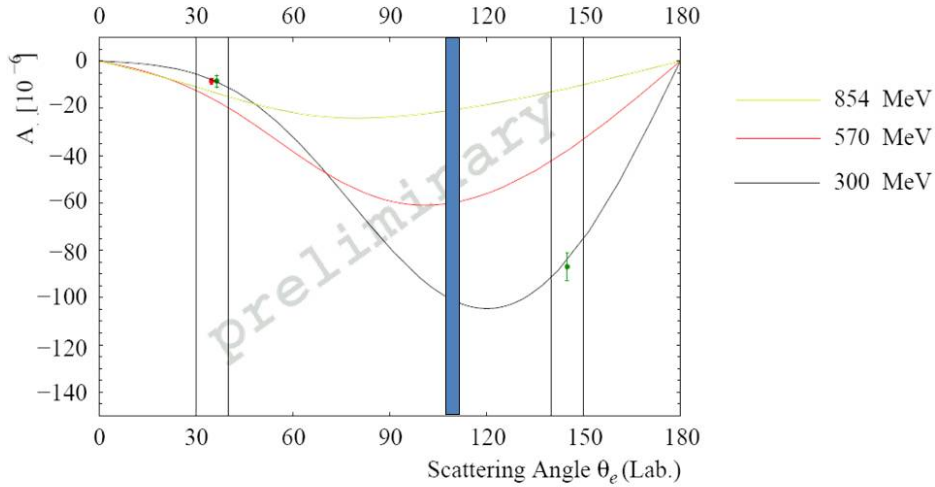


Figure 9: Theory calculation at different energies vs. lab scattering angle.

The estimate of the variation of the cross section with angle is $\frac{1}{\sigma} \frac{d\sigma}{d\theta} \sim 4\%/degree$. From the theory plot it can be estimated that the variation of the asymmetry with scattering angle $\frac{1}{A} \frac{dA}{d\theta} \sim -0.76\%/degree$ for 300 MeV and $\sim +0.16\%/degree$ at 570 MeV. Because of a miscommunication before the unblinding, the estimate of the asymmetry was made assuming a 3% variation in the yields around the mean, or $\frac{1}{4} \times 3\% \sim 1\%$ (taking the variation of the asymmetry with angle as the larger of the two or $\sim 1\%/degree$). But this is probably already an overestimate, so I am not sure it is necessary to actually use 2% instead of 1%.

For the purposes of the transverse asymmetry correction, what really matters is an

asymmetry between opposite octants. In order to actually apply a correction, we would need to know the nature of the detector asymmetry, and there is no reliable way to determine this from the data. Differences in yields from octant to octant could be for any number of reasons, some of which would be relevant to this detector asymmetry, such as a misplacement in radius or an actual variation in the magnetic field. Or the thresholds for the detectors could be different in that octant which would not be a detector asymmetry. Conversely there are effects that would impact the detector asymmetry but would not be reflected in the yields, such as a misplacement of the detectors in phi. More subtle would be a difference in the statistical contribution from octant to octant, which would affect the weighting of the asymmetries in an octant dependent manner. The use of the estimate of the detector asymmetry, A_S , using the variation in the yields from octant to octant is meant to provide an upper limit on how big the transverse correction could be.

3 Summary and Conclusion

The numbers in Table 3 are what was reported at the unblinding meeting. Those numbers were for the unblinded and uncorrected pass 4 asymmetries. These numbers will have to be updated and also need to be separated by wien angle setting. For now I thought it prudent to archive the methods and results here. As mentioned in section 2.3 this correction is not actually applied, but is included as an additional systematic uncertainty for each target/energy combination.

Dataset	A_T (ppm)	A_T^{lumi} (ppm)	A_L^{lumi} (ppm)	K_S (ppm)
H362	0.35 ± 0.04	23.5 ± 1.2	20.8 ± 18	0.022 ± 0.003
D362	-0.83 ± 0.02	23.2 ± 0.1	57.4 ± 68	0.036 ± 0.002
H687	0.74 ± 0.04	19.0 ± 0.3	150.5 ± 4.2	0.008 ± 0.007
D687	0.37 ± 0.02	18.2 ± 0.4	100.0 ± 6.1	0.012 ± 0.013

Table 3: Summary of the magnitude of the transverse correction in each dataset.

A Wien Angle Settings

The wien filter is used to account for the precession of the electron's spin as it goes through the bending magnets in the accelerator. There are no elements that would cause the spin to precess out of plane, although there may be some very small residual fields. So the precession occurs mostly in plane 10. In this example, the spin and velocity start out in the same direction, and the spin has precessed by an amount

$$\Delta\phi = \frac{g-2}{2} \frac{E}{m_e} \Delta\theta \quad (6)$$

where θ is the bend angle. There are two linacs and also a bend angle of $\sim -37^\circ$ going into the hall, so it is necessary to split the calculation into parts with a constant energy. In the case of the higher energy, both linacs were used, and they were set to about 325.2 MeV (and an injector energy of 36.6 MeV [4]). So in the first arc the precession was about 148° , but then the electrons were further accelerated in the south linac, so it is necessary to take that into account when calculating the precession into the hall, which is about 57° , for a total precession of 91° . In the case of the lower energy, only the north linac was used. So the precession of the electrons spin is $\sim 148^\circ$ through the first arc and $\sim 30^\circ$ in the hall arc, for a total precession of about 118° . In both the high and low energy the initial polarization was actually opposite the electron's momentum, so without the wien filter the polarizations would be roughly beam left, so in the higher energy the wien angle is set to $\sim 90^\circ$, and in the lower energy it is set to $\sim 70^\circ$ to get positive helicity in the hall with the polarization in the same direction as the electron's momentum. For the transverse polarization, the wien filter is set 90° lower so that the polarization is positive to beam left.

The wien angle settings were stored in epics data and written out in the logfiles. I wrote

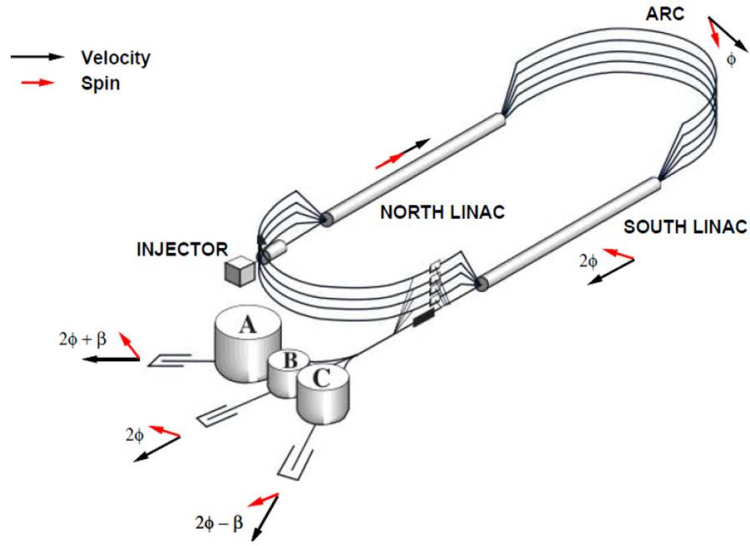


Figure 10: An example of how the spin precesses through the accelerator.

a routine to grep the settings from the log files and have summarized them here in table A.

Dates	Dataset	Polarization	Run Range	Wien Angle Setting
March '06 - April '06	H687a	Longitudinal	28330 - 29072	92.492
July '06 - August '06	H362	Longitudinal	29973 - 30795	71.224
July '06 - August '06	H362	Transverse	30803 - 30838	-18.97
July '06 - August '06	H362	Transverse	30839	-16.26
Sept. '06 - Oct. '06	H687b	Longitudinal	30992 - 31820	92.246
Sept. '06 - Oct. '06	H687b	Transverse	31350 - 31370	1.6959
Oct. '06 - Dec. '06	D687a	Longitudinal	31938 - 32551	92.246
Oct. '06 - Dec. '06	D687a	Longitudinal	32552 - 32565	90.844
Oct. '06 - Dec. '06	D687a	Longitudinal	32566 - 33040	90.043
Jan. '07 - Feb. '07	D362	Longitudinal	33143 - 34251	69.223
Jan. '07 - Feb. '07	D362	Transverse	33992 - 34018	-20.99
March '07	D687b	Longitudinal	34319 - 34454	90.549
March '07	D687b	Longitudinal	34459 - 34851	93.247
March '07	D687b	Transverse	34762 - 32765	1.1959

Table 4: Summary of the wien angle settings for each dataset.

References

- [1] The G^0 Experiment Backward Angle Measurements Update. The G^0 Collaboration. June 2005.
- [2] P. King, S.P. Wells, and the G0 Collaboration. Measurement of the vector analyzing power in e-p scattering using the G0 forward angle apparatus. G0 Document 437-v1. 2003
- [3] Pasquini, B. and M. Vanderhaeghen (2004). "Resonance estimates for single spin asymmetries in elastic electron-nucleon scattering." *Physical Review C* 70(4): 045206.
- [4] D. Gaskell. Private communication.
- [5] M. Pitt. Private communication.
- [6] J. Mammei. Presentation at the PAVI09 conference. June 2009